The effects of hydration on the topographical and mechanical properties of corneocytes

Évora, Ana S; Zhang, Zhibing; Johnson, Simon A; Adams, Michael J

DOI:
10.1016/j.jmbbm.2023.106296

Document Version
Publisher's PDF, also known as Version of record

Citation for published version (Harvard):
Évora, AS, Zhang, Z, Johnson, SA & Adams, MJ 2024, 'The effects of hydration on the topographical and mechanical properties of corneocytes', *Journal of the Mechanical Behavior of Biomedical Materials*, vol. 150, 106296. https://doi.org/10.1016/j.jmbbm.2023.106296

journal of the mechanical behavior of biomedical materials 150 (2024) 106296

Contents lists available at ScienceDirect

Journal of the Mechanical Behavior of Biomedical Materials

journal homepage: www.elsevier.com/locate/jmbbm

The effects of hydration on the topographical and mechanical properties of corneocytes

Ana S. Évora *, Zhibing Zhang, Simon A. Johnson, Michael J. Adams

School of Chemical Engineering, University of Birmingham, Birmingham, UK

ARTICLE INFO

Keywords:
Corneocyte
Stratum corneum
AFM
Relative humidity
Water activity
Hydration
Biomechanics

ABSTRACT

It is well established that the biomechanical properties of the Stratum Corneum (SC) are influenced by both moisture-induced plasticization and the lipid content. This study employs Atomic Force Microscopy to investigate how hydration affects the surface topographical and elasto-viscoplastic characteristics of corneocytes from two anatomical sites. Volar forearm cells underwent swelling when immersed in water with a 50% increase in thickness and volume. Similarly, medial heel cells demonstrated significant swelling in volume, accompanied by increased cell area and reduced cell roughness. Furthermore, as the water activity was increased, they exhibited enhanced compliance, leading to a decreased Young's modulus, hardness, and relaxation times. Moreover, the swollen cells also displayed a greater tolerance to strain before experiencing permanent deformation. Despite the greater predominance of immature cornified envelopes in plantar skin, the comparable Young's modulus of medial heel and forearm corneocytes suggests that cell stiffness primarily relies on the keratin matrix rather than on the cornified envelope. The Young's moduli of the cells in distilled water are similar to those reported for the SC, which suggests that the corneodesmosomes and intercellular lamellae lipids junctions that connect the corneocytes are able to accommodate the mechanical deformations of the SC.

1. Introduction

During certain body movements or in bedridden patients, human skin is subjected to large deformations causing potentially dangerous strains that may, ultimately, result in open wounds (Gefen et al., 2022; Kottner et al., 2020). The mechanical properties of the skin surface, the Stratum Corneum (SC), and sub-surface layers play a crucial role in resisting pressure and shear. The SC is usually described by a "bricks and mortar" structural model and, more recently, by the Kelvin's tetrakaidecahedron cell shape model, in which the corneocytes, its main cell type, are completely flattened and the keratin-filled interior is surrounded by cornified protein and lipid envelopes (CEs and CLEs). In this model, the cell shape provides a fundamental basis for the barrier homeostasis and physical strength of cornified stratified epithelia (Yokouchi et al., 2016). Adjacent corneocytes are connected by corneodesmosomes (CDs) and intercellular lamellae lipids, such as ceramides, cholesterol and fatty acids, which compose the "mortar" of the SC that surrounds corneocytes (Évora et al., 2021). Corneocytes are synthesized in the basal layer of the epidermis and mature into comparatively hard structures (Eckhart et al., 2013). Their stiffness arises from an internal network of keratin, a sulphur-containing fibrous protein embedded in a protein matrix and surrounded by a rigid cornified envelope. Park and Baddiel (1972a, b) have elegantly explored the mechanical changes occurring in the SC with relative humidity (RH), concluding that effective plasticization depends on the water content rather than the lipid content. Furthermore, there was a reduced water-retaining capacity of the SC upon extraction with organic solvents and followed by an aqueous extraction, due to the removal of hygroscopic substances, namely the natural moisturizing factor (NMF) (Park and Baddiel, 1972a).

The swelling of SC in water has been analysed by photographic recordings and determining the thickness by confocal laser scanning microscopy (Norlén et al., 1997). After 90 min of incubation in distilled water, the through-thickness swelling was 26.0 ± 16.3%. The authors argued that the results were consistent with the orientation of the keratin filaments, which results in cell rigidity and restricts lateral yielding.

Abbreviations: AFM, atomic force microscopy; SC, stratum corneum; CE, cornified envelope; CLE, cornified lipid envelope; PDMS, polydimethylsiloxane; RH, relative humidity; A_w, water activity.

* Corresponding author. School of Chemical Engineering, University of Birmingham, UK.
E-mail addresses: A.S.M.M.Evora@bham.ac.uk (A.S. Évora), z.zhang@bham.ac.uk (Z. Zhang), s.a.johnson@bham.ac.uk (S.A. Johnson), m.j.adams@bham.ac.uk (M.J. Adams).

https://doi.org/10.1016/j.jmbbm.2023.106296
Received 16 June 2023; Received in revised form 4 August 2023; Accepted 2 December 2023
Available online 7 December 2023

The swelling of individual corneocytes collected from the volar region of the forearm, close to the wrist, has also been studied using AFM in the tapping mode in air and in distilled water (Richter et al., 2004). There was an increase in both the volume and in the mean thickness of ~50 ± 10%, whereas significant lateral swelling was not observed. Additionally, the macroscopic swelling of corneocytes has been found to be replicated by the solvation and elasticity of helical tubes with a woven geometry in a computational model, equivalent to that of a keratin filaments arrangement (Evans and Roth, 2014). Norlén et al. then suggested that the morphology could be described as a cubic (para) crystalline polymer lattice, i.e., the keratin fibres being arranged isotropically possibly with chemical and/or physical attachment points between the fibres. This would ensure that all fibres contribute optimally to the enhanced stiffness and thereby distribute impact loads throughout the entire lattice, thus providing the SC with an optimal strength to weight ratio (Norlén, 2006).

Previous research has investigated the mechanical and topographical properties of the SC (German et al., 2012, Geerligs et al., 2011). It has also revealed links between water loss, percutaneous absorption, and corneocyte surface area, but these only partially explain permeability differences (Rogier, 1988). Traction force microscopy was used to investigate SC topographical features at different scales, influencing its overall mechanical properties including elastic modulus (Levi et al., 2010; Levi and Dauskardt, 2012). Finite element simulations explored the geometric effects on skin layers and mechanical responses (Leyva--Mendivil et al., 2015), emphasizing the importance of considering the 3D characteristics of human skin. Increased skin roughness correlates positively with skin condition (Murahata et al., 1984), and surface analysis helps evaluate cracks objectively (Murahata et al., 1984). However, the surface topography of skin cannot be directly related to single skin cells due to the different length scales of skin surface topography and AFM imaging. In fact, increased cell roughness in corneocytes has been associated with a disrupted skin barrier (Riethmuller et al., 2015). Liu's work highlights structural heterogeneities in the SC and the role of intercellular adhesion in failure under tensile stress (Liu et al., 2016). Wildnauer's study revealed the crystalline nature of the SC, cohesive agents, and fracture sites (Wildnauer et al., 1971).

Thus far, the effects of hydration on the biomechanical properties of superficial single skin cells have not been investigated. The aim of the present work was to evaluate the relationship between the hydration, surface topography, and mechanical properties of individual corneocytes collected from the forearm and medial heel of three healthy individuals using AFM.

2. Materials and methods

2.1. Corneocyte collection

Corneocytes were collected from three healthy female adult participants, with ages ranging from 26 to 31 years, in accordance with the UK regulations and the Declaration of Helsinki. Ethics approval was obtained from the University of Birmingham Research Ethics Committee – ERN-19-1398B. Samples were collected using the tape stripping method (Sellotape, UK) from two anatomical sites: forearm and medial heel (Lademann et al., 2009). The first layer of corneocytes was removed and discarded to avoid the presence of contaminants, such as clothing fibres. The second tape strip was used for the AFM measurements.

2.2. Atomic force microscopy

Atomic force microscopy (AFM) imaging and nanoindentation experiments were performed using AFM operated in Tapping Mode (TM) and Force Spectroscopy, respectively (Nanowizard 4, Bruker, JPK BioAFM Berlin, Germany). Standard imaging tips, with a nominal spring constant of 40 N/m and resonance frequency of 300 kHz, were used (NCHV-A, Bruker AFM Probes, Inc). The determination of the geometry of the AFM tips is described in Supplementary Information S1. Briefly, an elastomer (polydimethylsiloxane, PDMS) was used as a reference material for nanoindentation; the value of the Young's modulus of the PDMS was measured by micromanipulation (Zhang et al., 1999). The best-fit power law index (m) for PDMS AFM force curves varied with indentation depth and the cantilever. In fact, experimentally, a 2nd order polynomial with zero intercept appeared to provide a more satisfactory fit over the entire range of the loading curve, rather than a single power law. This indicated that the geometries of the probes were more closely approximated by a truncated cone than a single power law such as a paraboloid ($m = 1.5$). Consequently, force curves were analysed using a combination of a 6th order polynomial smoothing function and power law equations to obtain a tip-radius function, i.e., contact radius, a, as a function of contact depth, h_c (Supplementary Information S1). A 6th order polynomial was observed to reduce significant systematic deviations and provided a smoother fit for the entire loading curve.

Corneocytes were extracted by pressing the tape onto a microscope glass slide and incubating overnight in xylene. Cells collected from participant 1 that were attached to the glass slide were imaged for surface topographical analysis, as well as for cell area, thickness and volume calculations (512 × 512 pixels, 50 × 50 μm). 10 cells were analysed per site. Moreover, forearm and medial heel cells of the three participants were analysed by AFM nanoindentation. This consisted of the analysis of 64 force curves (indentation force, F, as a function of the indentation depth, h) extracted from 8 × 8 matrices, with points spaced 625 nm apart, and involved loading-pause-unloading cycles. Stress-relaxation was studied over a 4 s pause period, after the maximum force setpoint at loading was reached. The pause segment was set at constant height and the force relaxation was measured. For each corneocyte, the maximum force setpoint was adjusted by ensuring that the maximum indentation depth was not greater than 10% of the cell thickness (≤1 μm) to avoid artifacts arising from the supporting substrate (Garcia and Garcia, 2018) (see Supplementary Information S4). The maximum applied force was 2 μN or 50 nN in air and in liquid, respectively, to obtain similar indentation depths ranging between 30 and 100 nm (see Fig. S2 in Supplementary Information S2).

To study the effects of hydration on the mechanical properties of single cells, measurements were performed in the nominally dry state (25 °C and 35% RH) and by incubating the samples in different glycerol-water solutions with decreasing glycerol concentration (w/w): 85, 70, 50 and 0% glycerol in distilled water, which corresponded to increasing values of water activity, A_w, of 0.42, 0.62, 0.8, 1 respectively (Nakagawa and Oyama, 2019). The maximum concentration of glycerol was limited to 85% since at greater concentrations the viscosity was too high for the AFM measurements. Measurements were performed for a total of 6 cells per participant and per condition after equilibrating the system for 20 min before measurements.

2.3. AFM data analysis

2.3.1. Elastic deformation

The Young's modulus, of the corneocytes was calculated from the unloading curves using the Oliver-Pharr method (Oliver and Pharr, 1992):

$$E = \frac{\sqrt{\pi}}{2}\left(1-\nu^2\right)\frac{S_0}{\sqrt{A}} \quad (1)$$

where S_0 is the stiffness at the maximum force, F_{max}, which corresponds to the maximum indentation depth, h_{max} , and $A=\pi a^2$ is the contact area, where a is the contact radius (Popov et al., 2019). The Poisson's ratio for corneocytes, ν, was assumed to be 0.4, based on the value for keratin (Hu et al., 2010). Prior studies using uniaxial tensile measurements have shown that the Poisson's ratio for human SC varies with hydration level, being about 0.25 at 40% RH and 0.47 for 100% RH

(Liu et al., 2016). However, this study considered isolated SC composed of corneocytes and intercellular lipids, which have been shown to influence the mechanical properties (Liu and German, 2015). Since in the current study nanoindentation experiments were performed on single corneocytes, the Poisson's ratio for corneocytes was assumed to be 0.4, based on the value for keratin, which is expected to be the main contributor to the mechanical behaviour of single corneocytes (Hu et al., 2010).

Corneocytes are elastoplastic materials (Beard et al., 2013), so that the contact depth is related to h_{max} by the expression (Oliver and Pharr, 1992):

$$h_c = h_{max} - h_s \tag{2}$$

where h_s is the surface elastic deflection at the perimeter of the contact, which is given by the following expression (Oliver and Pharr, 1992):

$$h_s = \varphi \frac{F_{max}}{S_0} \tag{3}$$

The unloading stiffness, $S_0 = dF/dh$ at $h{=}h_{max}$ was obtained by differentiating the following polynomial fit to the upper 80% of the unloading curve and determining the slope at h_{max} (Fischer-Cripps, 2002):

$$F = C_e h^2 - \left(2C_e h_f\right)h + C_e h_f^2 \tag{4}$$

where C_e and h_f are fitting parameters. The geometric factor, φ, was assumed to be 0.73 for a conical indenter, following the work of Oliver and Pharr (2004).

The tip contact radius functions, $a(h_c)$, for all the tips employed in this study are shown in Fig. S1 (Supplementary Information S1). These functions are required to calculate the contact area for each indent at h_{max} in Eq. (1) from the contact depth obtained using Eqs (2) and (3).

2.3.2. Force-relaxation analysis

The time-dependent properties of the corneocytes were calculated by fitting the following Prony series to the force-relaxation curves:

$$F(t) = B_0 + B_1 e^{-t/\tau_1} + B_2 e^{-t/\tau_2} \tag{5}$$

from which the coefficients B_0, B_1 and B_2 were obtained, as well as the characteristic relaxation times, τ_1 and τ_2. Assuming the decay in the force arises from viscoplastic dissipation, the force can be related to the time-dependent hardness $H(t) = F(t)/A$:

$$F(t){=}\pi a^2 H(t) \tag{6}$$

and thus,

$$H(t) = C_0 + \sum_{i=1}^{2} C_i e^{-t/\tau_i} \tag{7}$$

so that the coefficients C_0, C_1 and C_2 can be calculated by:

$$C_i{=}\frac{B_i}{\pi a^2} \tag{8}$$

where $i = (0, 1, 2)$. Finally, the instantaneous hardness, H_0 and the steady state hardness, H_∞, can then be estimated using the following relationships:

$$H_0 = \sum_{i=0}^{2} C_i \tag{9}$$

and

$$H_\infty{=}C_0 \tag{10}$$

2.3.3. Statistical analysis

Raw data were imported into IBM® SPSS® Statistics (version 27) for analysis and assessed for normality using probability plots and the Shapiro-Wilk test for each site and participant. Two-way ANOVA followed by Dunnett's multiple comparisons test was employed to investigate whether there were differences in the topographical and mechanical properties of the cells with different values of A_w. Moreover, paired t-student tests were applied to investigate differences in relaxation times between the dry state and that in distilled water. Tests were considered statistically significant at a 5% level ($p < 0.05$). All tests were two-tailed.

3. Results

3.1. The effects of hydration on the topographical features of corneocytes

Typical topographical images of volar forearm and medial heel corneocytes obtained under ambient conditions and incubated in distilled water are shown in Fig. 1. Each image represents the map of cell surface heights relative to the underlying glass substrate and is analysed to give the cell dimension values summarised in Table 1.

Forearm corneocytes under ambient conditions (nominally dry state of 35% RH) presented a relatively rough surface, characterized by ridges across the surface, organized in peaks and valleys (Fig. 1a). Villi-like features were observed on the surface of medial heel cells (Fig. 1c). Forearm and medial heel cells incubated in distilled water showed a less corrugated surface (Fig. 1b and d), with a decrease in surface roughness of $\sim$ 30 and 50% ($p < 0.01$), respectively. Furthermore, swelling was observed for forearm cells as an increase in the volume ($\sim$ 63%, $p < 0.05$) and mean thickness ($\sim$ 52%, $p < 0.05$), but significant lateral swelling was not observed (Table 1). Similar swelling was found for medial heel cells, with an increase of $\sim$20% in thickness, $\sim$ 50 ($p < 0.01$) in volume, and a similar trend was observed for the cell area ($\sim$ 14%, not statistically significant).

3.2. The effect of hydration on the biomechanical properties of corneocytes

The Young's moduli of the corneocytes as a function of the nominal water activity are presented in Table 2, and Figs. 2 and 3. Forearm and medial heel cells presented mean moduli of 620 and 560 MPa in the nominally dry state (35% RH), with mean values of the instantaneous hardness of 210 and 160 MPa for the forearm and medial heel cells, respectively. The corresponding steady state mean hardness values were 180 and 140 MPa, respectively.

With increasing water activity, a clear decrease in the individual modulus values was observed for all participants and both anatomical sites studied (Figs. 2 and 3). For example, cells in 85% glycerol (A_w = 0.42) displayed much smaller moduli of about 6–7 MPa compared to those of the dry state (35% RH), which were in the range 560–620 MPa. Cells became even softer when incubated in distilled water (A_w = 1), with Young's moduli of about 1.5–2 MPa ($p < 0.001$, Table 2). The same trends were observed for the instantaneous and long-term hardness values, i.e., there was a decrease in hardness with increasing water activity ($p < 0.001$). Moreover, there was a faster relaxation time (τ_2) when the cells were incubated in distilled water (Fig. 3c and d), compared to the dry state (35% RH). There was also a trend for an increase in the yield strain ($\epsilon_Y = H_0/E$) with increasing water activity, particularly for $A_w > 0.62$ (Table 2).

The Herschel-Bulkley model (Saramito, 2009) was also applied to the rate-dependent data to characterize the material properties according to the hydration level (the details are given in the Supplementary Information S3 and Table S2), which may be expressed as:

$$\sigma = \sigma_Y + k\left(d\varepsilon_p / dt\right)^j \tag{11}$$

where σ_Y is the quasi-static uniaxial yield stress, k is the plastic flow consistency and j is plastic flow index. The value of j was found to be < 1 for all conditions studied ($\sim$ 0.4–0.5) (Table S2) and approximately

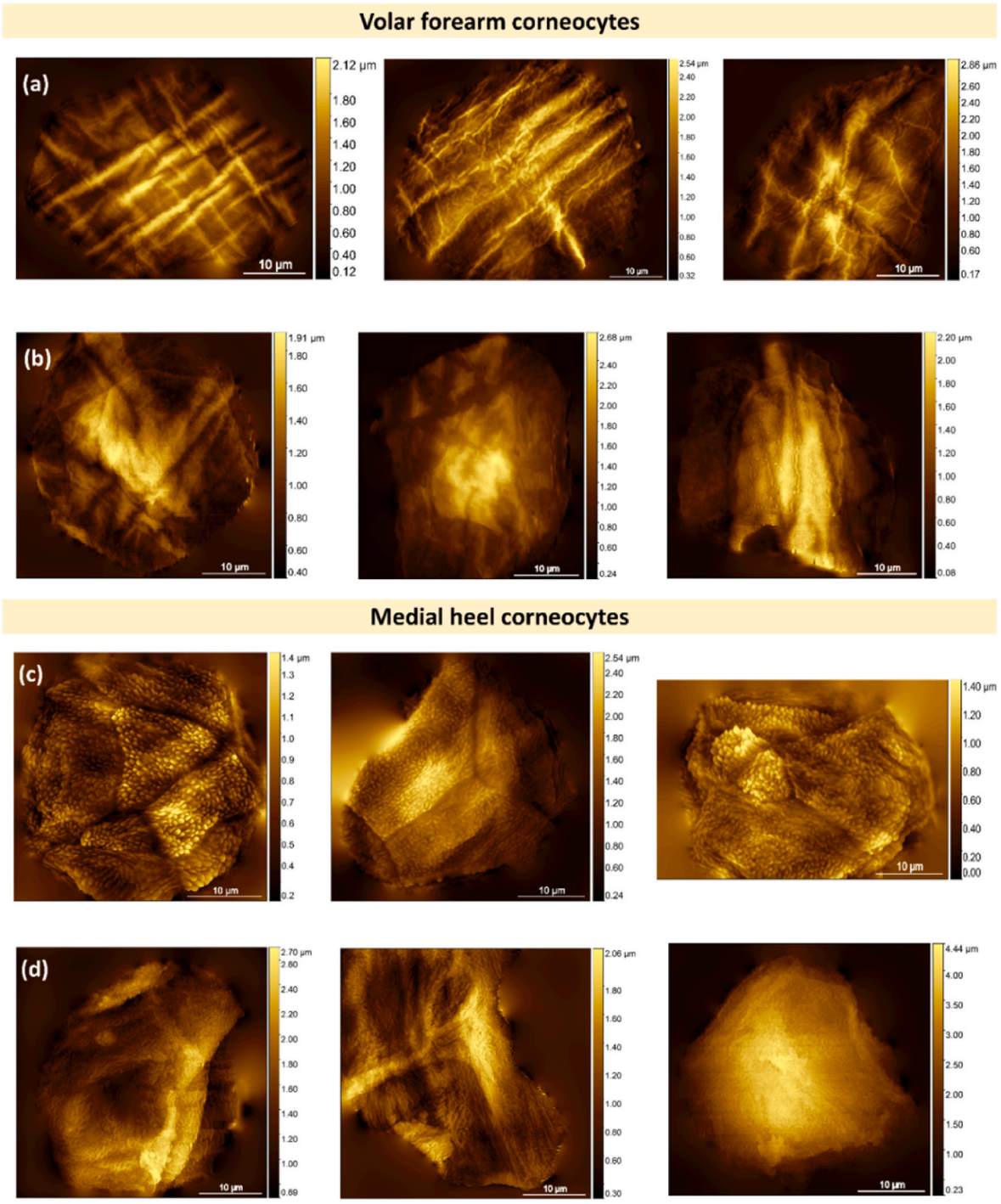

Fig. 1. TM images of volar forearm and medial heel corneocytes. (a and c) Cells under ambient conditions. **(b and d)** Cells in distilled water. The mean thickness increases from 0.8 ± 0.2 μm and 1.1 ± 0.3 μm in the dry state to 1.14 ± 0.3 μm and 1.3 ± 0.3 μm in water, for forearm and medial heel cells respectively. The scan size in both sets of images was 50 μm × 50 μm. Scale bar = 10 μm.

independent of A_w. However, there was a decrease in the quasi-static uniaxial yield stress ($\sigma_Y \sim$ 30–40 MPa in the nominally dry state, down to 0.30–0.40 and 0.12–0.14 MPa when $A_w = 0.42$ and 1, respectively). Moreover, there was also a decrease in k with increasing A_w, viz., $\sim$ 20 MPa s^j in the nominally dry state and 0.2–0.3 MPa s^j when $A_w =$ 0.42, and $\sim$ 0.10 MPa s^j in distilled water (Table S2).

4. Discussion

This is the first study of the effects of hydration on both the surface topographical and biomechanical properties of single superficial corneocytes. Specifically, it involved the effects of water activity on the Young's modulus, hardness and relaxation times of volar forearm and medial heel corneocytes, which were studied in the nominally dry state and by equilibrating them in aqueous solutions of different glycerol concentrations and in distilled water. Volar forearm corneocytes were found to swell when immersed in distilled water (~50%, Table 1). A similar swelling of ~50% has been previously observed for corneocytes from the forehand (close to the wrist) in distilled water (Richter et al., 2004), as well as for the most superficial layers of the SC (Richter et al.,

Table 1
Thickness, area, volume, and surface roughness (S_q) measured for corneocytes in air and distilled water. Data are expressed as mean ± 1 SD based on measurements of 10 random cells for each condition and a single participant. *p < 0.05, **p < 0.01 in *t*-test performed for each parameter. The mean proportional change in water compared to the measurements under ambient conditions is given as a percentage.

Corneocyte parameter	Air (35% RH)		Distilled Water		Mean Change %	
	Forearm	Medial Heel	Forearm	Medial Heel	Forearm	Medial Heel
Thickness (μm)	0.8 ± 0.1	1.1 ± 0.2	1.1 ± 0.3	1.3 ± 0.3	+52*	+21
Area (μm^2)	1084 ± 128	745 ± 70	1041 ± 201	851 ± 147	−4	+14
Volume (μm^3)	819 ± 135	850 ± 172	1337 ± 408	1283 ± 223	+63*	+50**
Root mean square height, S_q (nm)	68 ± 22	138 ± 40	47 ± 11	68 ± 10	−30	−50**

Table 2
Mechanical properties of forearm and medial cells with hydration. (There were 3 participants and 6 cells per participant, mean ± SD).

Hydration level		E (MPa)		H_0 (MPa)		$H\infty$ (MPa)		τ_1 (s)		τ_2 (s)		$\varepsilon_Y = H_0/E$	
		Forearm	Medial Heel	Forearm	Medial Heel	Forearm	Medial Heel	Forearm	Medial Heel	Forearm	Medial Heel	Forearm	Medial Heel
Air (RH)	**35%**	620 ± 320	564 ± 59	214 ± 90	161 ± 46	178 ± 79	139 ± 44	0.09 ± 0.02	0.08 ± 0.01	1.33 ± 0.46	1.26 ± 0.15	0.37 ± 0.12	0.29 ± 0.10
85% (A_w)	**0.42**	6.9 ± 2.0	6.2 ± 0.9	2.1 ± 0.6	2.8 ± 1.3	0.9 ± 0.2	1.0 ± 0.4	0.09 ± 0.05	0.07 ± 0.01	0.87 ± 0.28	0.76 ± 0.03	0.32 ± 0.11	0.46 ± 0.20
70% (A_w)	**0.62**	2.1 ± 1.1	3.3 ± 1.5	0.9 ± 0.2	1.9 ± 1.2	0.4 ± 0.1	0.5 ± 0.2	0.12 ± 0.06	0.11 ± 0.03	1.14 ± 0.26	0.85 ± 0.12	0.55 ± 0.19	0.64 ± 0.44
50% (A_w)	**0.80**	1.8 ± 0.2	1.8 ± 0.9	0.8 ± 0.2	1.1 ± 0.5	0.4 ± 0.1	0.4 ± 0.2	0.06 ± 0.01	0.07 ± 0.01	1.06 ± 0.15	1.03 ± 0.09	0.45 ± 0.10	0.61 ± 0.26
H_2O (A_w)	**1.00**	1.4 ± 0.1	1.5 ± 0.8	0.8 ± 0.2	1.3 ± 0.7	0.4 ± 0.1	0.5± 0.3	0.04 ± 0.01	0.07 ± 0.01	0.70 ± 0.03	0.78 0.10	0.58 ± 0.20	0.87 ± 0.42

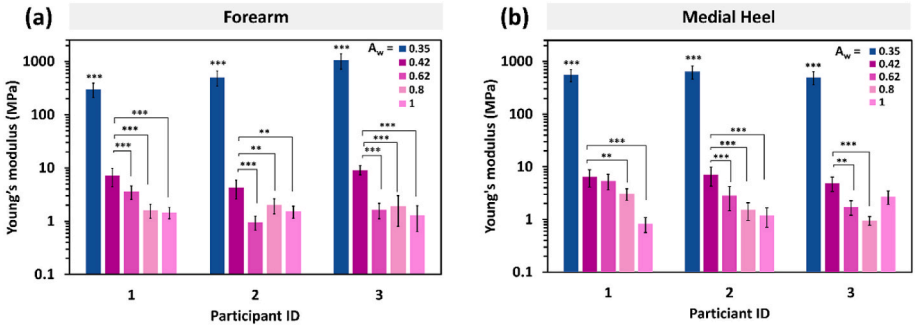

Fig. 2. Young's moduli of corneocytes. (a) Volar forearm and **(b)** medial heel corneocytes collected from three healthy individuals in the dry state (blue) and immersed in aqueous glycerol solutions with a range of water activities. There were 6 cells per participant per condition. **< 0.01, ***p < 0.001 based on a two-way ANOVA followed by Dunnett's multiple comparisons test.

2004). Interestingly, the swelling in medial heel cells was observed as an increase in volume (~50%, p < 0.01) and thickness (~20%, not statistically significant), but also in cell area (~14%, not statistically significant). This was accompanied by a decrease in cell roughness (~50%), which indicates that the swelling of medial heel cells might depend on the flattening of the villi-like structures, with enlargement of the cell area. This smaller increase in thickness, compared to forearm corneocytes, may be related to differences in structure and compositions such as the type of keratin expressed in palmoplantar skin. In fact, while keratins 1 and 10 are expressed in non-glabrous skin, palmoplantar epidermis structural integrity depends on keratin 9 (Fu et al., 2014), which was suggested to interact with keratin 5, instead of keratin 1 (Fu et al., 2014). Future research should investigate the interactions and structure of keratin 9 filaments in palmoplantar skin in order to understand if the keratin matrix architecture and swelling are similar to those in non-glabrous skin.

Corneocytes become more compliant with increasing A_w, such that the values of the Young's modulus decrease from hundreds of MPa in the nominally dry state (~ 630 MPa) to a few MPa when in distilled water (~ 1.5–2 MPa). This is accompanied by a decrease in the instantaneous and long-term hardness values (~ 160–215 and 140–180 MPa, down to 0.8–1.3 and 0.4–0.5 MPa, respectively), as well a decrease in the second relaxation time, τ_2, (1.3 s in the dry state down to 0.8 s in the wet state). Moreover, the yield strain tended to increase with an increase in A_w, from about 0.30 to 0.40 in the dry state (35% RH) up to 0.6–0.9 in distilled water. That is, the swollen cells can accommodate larger strains before undergoing permanent deformation since they are considerably more compliant.

Previously, Park and Baddiel (1972a) studied the dependence of the mechanical properties of the SC (isolated from pig ears) on the relative humidity using an extensometer. The Young's modulus was found to be ~2 GPa, at 30% RH and 25 °C, while at 100% RH, it decreased to ~3 MPa. They concluded that this was a result of a glassy-rubbery transition. At low RH values, the SC could be described as a polymeric glass, where long chain movements are restricted, and extension takes place by the stretching of bonds. They argued that in the wet state, bond scission of the hydrogen bonds and salt linkages occurs due to hydration, but disulphide bonds remain intact, and thus the SC protein chains form a sparse cross-linked entanglement network that is similar to an elastomer. This could explain the behaviour of single corneocytes, whose mechanical properties may depend upon the main component, keratin. In fact, different studies have proposed the importance of the cornified envelope (CE) in maintaining cell rigidity and integrity (Guneri et al., 2018; Park and Baddiel, 1972a, 1972b). However, in a previous study we were not able to establish a relationship between cell stiffness and CE maturity, i.e., although medial heel cells presented higher levels of immature CEs compared to the forearm, significant differences were not observed for the Young's modulus or the yield stress (Évora et al., 2023). This may be interpreted in two possible ways: i) the CE, even if contributing to the mechanical architecture of corneocytes, is not fundamental in ensuring the mechanical strength of the cell; ii) although medial heel samples exhibited high levels of immature CEs (Évora et al., 2023), their CE rigidity is similar to that of forearm cells. The later possibility arises from previous observations that the immunostaining

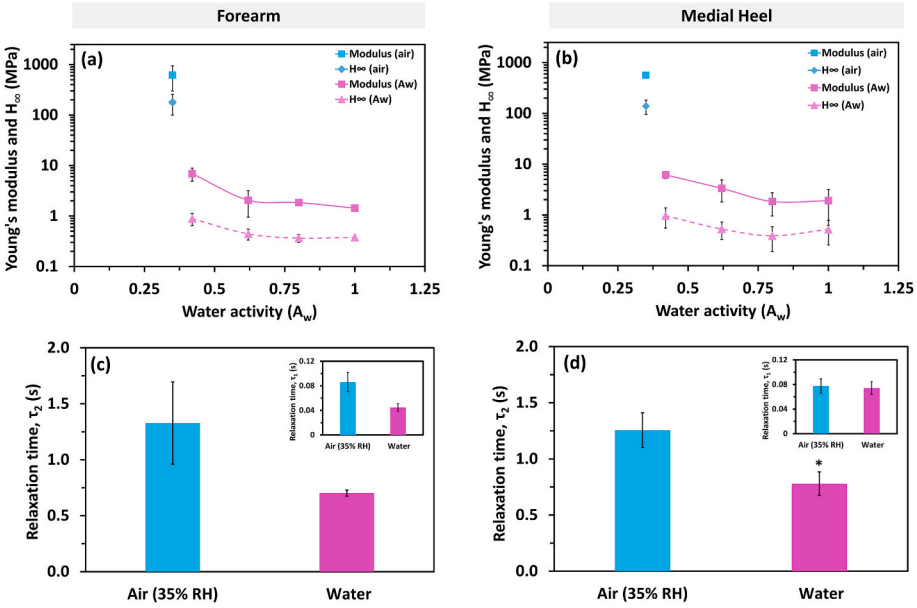

Fig. 3. A decrease in the Young's modulus and long-term hardness, H_∞, was observed for volar forearm and medial heel corneocytes when exposed to increasing water activity. This was confirmed by two-way ANOVA followed by Dunnett's multiple comparisons test against the dry state (35% RH) and the lowest A_w (85% glycerol), respectively ($p < 0.05$). The results are presented as mean ± 1 SD based on three healthy participants. *$p < 0.05$ paired t-student test to compare relaxation times between dry and wet state.

method used to analyse CE maturity depends on the hydrophobicity, not on the mechanical properties. In fact, it is possible that medial heel CEs are equally as stiff as forearm cells, but do not display the typical cornified lipid envelope present in mature non-glabrous SC (Évora et al., 2021; Guneri et al., 2018).

Interestingly, a correlation between the level of CE maturity and the Young's modulus for forearm cells has been observed (Évora et al., 2023), i.e., subjects with greater levels of CE maturity presented generally stiffer cells. This could explain the inter-subject variability found in the current study (Table 2). Nonetheless, the absence of a more radical effect of CE maturity on the Young's modulus of corneocytes, might indicate that keratin is indeed mainly responsible for the mechanical properties of the cells, and thus, for the SC stiffness. However, a rigid CE, compared to the typical phospholipidic cell membrane of keratinocytes, might be fundamental towards maintaining cell integrity when cells swell in liquid and towards resisting chemical-induced stresses, such as detergents. In fact, a highly cross-linked and insoluble protein membrane, such as the CE, is more equipped to resist dissolution and denaturation by certain detergents, e.g., sodium dodecyl sulphate, and to resist osmotic pressures induced by cell swelling in water.

Park and Baddiel (1972c) also studied the effects of A_w on the Young's modulus of the SC, using saturated salt solutions. The mean modulus at small values of $A_w = 0.42$ (85% glycerol) for corneocytes (6–7 MPa), was much smaller than that of the SC (of ~200 MPa) (Park and Baddiel, 1972c). This may be due to the humectant ability of glycerol aqueous solutions, but not of the saturated salt solutions in native SC (Park and Baddiel, 1972c), to effectively wet the cells (Björklund et al., 2014). In fact, native SC retains the lipid lamellae, which acts as a barrier, while, in this study, corneocytes are being studied after xylene extraction, which may have dissolved any extracellular lipids attached to the cell surface. Interestingly, the Young's modulus of the SC in water (~5 MPa) was close to that of corneocytes (1.5–2 MPa) (Park and Baddiel, 1972c). Prior research has investigated the moisturizing capabilities of glycerol during the drying process of the SC (Liu et al., 2016). It was observed that glycerol treatments led to reductions in the elastic modulus after drying and in the maximum drying stresses in both the reference SC and the barrier disrupted SC (lacking intercellular lipids). While our study did not examine the moisturizing effects of glycerol on corneocyte properties, these previous findings may explain the relatively small moduli observed in samples treated with various glycerol solutions, including the one with the smallest *Aw* (0.42) of 85% glycerol.

While in the current work, single corneocytes were studied through nanoindentation, the properties of the SC have been typically measured using an extensometer, and thus the effects of the cell-to-cell junctions (CDs) on the mechanical resilience of the layer cannot be ignored. However, the similar values of Young's moduli obtained in water for single corneocytes, and an SC layer suggest that the lipid mortar and corneodesmosomes do not seem to restrict significantly the deformability of the SC. Moreover, previous studies have investigated the effects of moisturization and barrier disruption on the dynamic drying of the SC (Liu et al., 2016). Those authors observed an increase in the elastic modulus, from initial values of 10 MPa up to about 25 MPa after 15 h of drying time. Interestingly, barrier disrupted SC presented an initial modulus of about 40–50 MPa, that increased up to about 100 MPa, after only 2 h of drying. When the SC was incubated with glycerol prior to the drying period, a decrease in Young's modulus was observed in both cases and with a much smaller increase after drying (less than 10 MPa for native SC and up to 50 MPa for barrier disrupted SC). The modulus values calculated for the SC at 99% RH in this study are similar to those found for single corneocytes incubated in water calculated in the current study. This provides another indication that, at least in the in-plane direction, cell-to-cell junctions do not seem to restrict the deformability of the SC when hydrated. The mechanical properties of isolated SC have also been studied using nanoindentation (Bhushan, 2012, Yuan and Verma, 2006; Geerligs et al., 2011). They found much smaller values of the Young's modulus, compared to those obtained for single corneocytes in the current study. In one example, isolated SC was observed to have a Young's modulus in the range of 1–2 MPa at 28% RH (Geerligs et al., 2011), while in another it was found to be about 100 MPa (Yuan and Verma, 2006). The disagreement between the moduli reported in these studies and single corneocytes may be related to differences in the protocols followed, for example by the use of a soft substate (double sided tape) that can have high compliance (Yuan and Verma, 2006). Interestingly, relatively similar values of Young's modulus were found for the case of wet SC (about 10 MPa) compared to single corneocytes (Yuan and Verma, 2006).

The current study was limited by the number of participants (3) and by using glycerol to vary the water activity, instead of the more commonly used saturated salt solutions. This was due to the high ionic strength of these solutions which prevented accurate AFM measurements due to the high electrostatic interaction interfering with the AFM tip. Although glycerol is not considered a skin plasticizer, in using it to control water activity the behaviour observed may not be fully attributable to the water activity since it may also be dependent on the humectant properties of glycerol (Björklund et al., 2014; Chen et al., 2022). Glycerol was shown to increase molecular mobility of keratin at a given RH, which could not be attributed to an increase in water content (Björklund et al., 2014). However, given the equipment used in the current work, it was not possible to measure the effects of relative humidity, which is expected to be different from that of incubating cells directly in liquid media. This may explain the large reduction between the dry state (equivalent to $A_w = 0.35$) and the solution of 85% glycerol ($A_w = 0.42$) (Fig. 3 and Table 2). The effects of relative humidity are expected to be less abrupt, considering the results obtained for the SC (Park and Baddiel, 1972a). In saturated salt solutions, the Young's modulus of the SC was observed to fall for values of <100 MPa when $A_w \sim 0.50$, while in the vapour phase, a similar drop is observed when the relative humidity is greater than 80% (Park and Baddiel, 1972b). The current study was also limited to two anatomical sites, and particularly the use of the volar forearm. This site can be subjected to the effects of UV radiation, which are known to be damaging to the SC structure, particularly by degrading corneodesmosomes (Lipsky and German, 2019). Consequently, future research should investigate the mechanical properties of other of anatomical sites such as the sacrum in order to obtain a clearer understanding of the mechanical behaviour of skin exposed and unexposed to the environment, and particularly to UV radiation.

It is also suggested that future studies should investigate the effects of relative humidity on the properties of corneocytes and particularly the relationship to the amount of natural moisturizing factor (NMF). It is proposed that the inter-subject variability found in the mechanical properties of the cells in the nominally dry state, apart from being partly correlated to CE maturity, is extremely dependent on the level of NMF, which is known to vary according to age (Du et al., 2013), anatomical site (Takada et al., 2012), and in diseases such as Atopic Dermatitis (Riethmuller et al., 2015). The levels of these compounds may be controlling the properties of corneocytes in varying RH environments since they are responsible for retaining water inside the cells. However, this could not be investigated with the protocol followed in the current study since any incubation in liquid media may extract the small NMF molecules and so mask their effect in native SC. Finally, the study of the rate-dependent properties and the calculation of the Herschel-Bulkley parameters (see Supplementary Information S3 suggest that the plasticization of corneocytes by water decreases the resistance to flow, becoming less viscous and less resistant to deformation under shear which has been observed for hair, another keratinous material (Yu et al., 2017). As discussed for SC, plasticization by water causes a rubbery-glassy transition, which results in a reduction in the Young's modulus and the yield stress but an increase in the yield strain.

5. Conclusions

Moisture plays a crucial role in the structure of the SC, assisting in the maintenance of the natural desquamation process by promoting the activity of serine proteases responsible for the degradation of corneodesmosomes (Watkinson et al., 2001). It also promotes the maturation of corneocytes (rigidity and hydrophobicity) (Guneri, 2020; Hirao, 2003). In the present study, corneocytes were found to swell in water by about 50% of their initial dry volume (Fig. 1 and Table 1) and to become much more compliant with increasing water activity (the Young's modulus was ~ 630 MPa in the nominally dry state and decreased to 1.5–2 MPa in distilled water). This indicates that, when hydrated, corneocytes contribute to the flexibility and softness of the SC, with the cells becoming more capable of withstanding deformation without breaking or undergoing structural damage as reflected in an increase in the yield strain. However, prolonged water exposure has been observed to disrupt the lipid lamellae structure with "water pools" being formed in the SC after several hours of water exposure (Warner et al., 2003). The expansion of the extracellular spaces between corneocytes and their swelling may weaken the structure of the corneodesmosomes, leading to impaired cell-to-cell adhesion (Hirao, 2003). This increases transepidermal water loss (Fluhr et al., 1999) and renders the skin surface more susceptible to the penetration of environmental irritants and microorganisms (Falloon et al., 2018). Therefore, hydration seems to play a dual opposing role in the SC. While being very important in promoting a healthy skin barrier and mechanical resistance in the wet state, prolonged exposure to moisture may be disruptive for the SC structure. Further studies should investigate the effects of prolonged exposure on both the mechanical properties of corneocytes, but also on the cell-to-cell adhesion. By fully characterizing the mechanical resistance of the SC under such conditions, it should be possible to gain a comprehensive understanding of the impact of prolonged hydration on skin health.

Funding

This work was supported by the European Union's Horizon 2020 research and innovation programme under the Marie Skłodowska-Curie grant agreement No. 811965 (Project STINTS - Skin Tissue Integrity under Shear).

CRediT authorship contribution statement

Ana S. Évora: Conceptualization, Data curation, Formal analysis, Investigation, Methodology, Software, Writing – original draft, Writing – review & editing. **Zhibing Zhang:** Conceptualization, Funding acquisition, Methodology, Supervision, Writing – review & editing. **Simon A. Johnson:** Conceptualization, Formal analysis, Methodology, Writing – review & editing. **Michael J. Adams:** Writing – review & editing, Conceptualization, Funding acquisition, Supervision.

Declaration of competing interest

The authors declare that they have no known competing financial interests or personal relationships that could have appeared to influence the work reported in this paper.

Data availability

Data will be made available on request.

Acknowledgments

The authors wish to thank all the participants who engaged with the study.

Supplementary data

Supplementary data to this article can be found online at https://doi.org/10.1016/j.jmbbm.2023.106296.

References

Beard, J.D., Guy, R.H., Gordeev, S.N., 2013. Mechanical tomography of human corneocytes with a nanoneedle. J. Invest. Dermatol. 133, 1565–1571.

Björklund, S., Andersson, J.M., Pham, Q.D., Nowacka, A., Topgaard, D., Sparr, E., 2014. Stratum corneum molecular mobility in the presence of natural moisturizers. Soft Matter 10, 4535–4546.

Bhushan, B., 2012. Nanotribological and nanomechanical properties of skin with and without cream treatment using atomic force microscopy and nanoindentation. J. Colloid Interface Sci. 367, 1–33.
Chen, H.J., Lee, P.Y., Chen, C.Y., Huang, S.L., Huang, B.W., Dai, F.J., Chau, C.F., Chen, C. S., Lin, Y.S., 2022. Moisture retention of glycerin solutions with various concentrations: a comparative study. Sci. Rep. 12, 10232.
Du, J.-X., Zhai, C.-M., Ye, Y.-Q., 2013. Face aging simulation and recognition based on NMF algorithm with sparseness constraints. Neurocomputing 116, 250–259.
Eckhart, L., Lippens, S., Tschachler, E., Declercq, W., 2013. Cell death by cornification. Biochim. Biophys. Acta 1833, 3471–3480.
Evans, M.E., Roth, R., 2014. Shaping the skin: the interplay of mesoscale geometry and corneocyte swelling. Phys. Rev. Lett. 112, 038102.
Évora, A.S., Adams, M.J., Johnson, S.A., Zhang, Z., 2021. Corneocytes: relationship between structural and biomechanical properties. Skin Res. Technol. 29, e13507.
Évora, A.S., Johnson, S.A., Zhang, Z., Adams, M.M., 2023. Characterization of Topographical, Biomechanical and Maturation Properties of Corneocytes with Respect to Anatomical Location. Submitted to peer review.
Falloon, S.S., Abbas, S., Stridfeldt, C., Cottenden, A., 2018. The impact of microclimate on skin health with absorbent incontinence product use: an integrative review. J. Wound Ostomy Cont. Nurs. 45.
Fischer-Cripps, A.C., 2002. Contact mechanics. In: Nanoindentation. Springer, New York, NY, pp. 1–19.
Fluhr, J.W., Lazzerini, S., Distante, F., Gloor, M., Berardesca, E., 1999. Effects of prolonged occlusion on stratum corneum barrier function and water holding capacity. Skin Pharmacol. Appl. Skin Physiol. 12, 193–198.
Fu, D.J., Thomson, C., Lunny, D.P., Dopping-Hepenstal, P.J., McGrath, J.A., Smith, F.J. D., Irwin McLean, W.H.I., Leslie Pedrioli, D.M., 2014. Keratin 9 is required for the structural integrity and terminal differentiation of the palmoplantar epidermis. J. Invest. Dermatol. 134, 754–763.
Garcia, P.D., Garcia, R., 2018. Determination of the elastic moduli of a single cell cultured on a rigid support by force microscopy. Biophys. J. 114, 2923–2932.
Gefen, A., Brienza, D.M., Cuddigan, J., Haesler, E., Kottner, J., 2022. Our contemporary understanding of the aetiology of pressure ulcers/pressure injuries. Int. Wound J. 19, 692–704.
Geerligs, M., van Breemen, L., Peters, G., Ackermans, P., Baaijens, F., Oomens, C., 2011. In vitro indentation to determine the mechanical properties of epidermis. J. Biomech. 44, 1176–1181.
German, G.K., Engl, W.C., Pashkovski, E., Banerjee, S., Xu, Y., Mertz, A.F., Hyland, C., Dufresne, E.R., 2012. Heterogeneous drying stresses in stratum corneum. Biophys. J. 102, 2424–2432.
Guneri, D., 2020. The Development and Validation of Novel Biomarkers to Assess the Skin Barrier Function. PhD Thesis. of University College London, UK.
Guneri, D., Voegeli, R., Gurgul, S.J., Munday, M.R., Lane, M.E., Rawlings, A.V., 2018. A new approach to assess the effect of photodamage on corneocyte envelope maturity using combined hydrophobicity and mechanical fragility assays. Int. J. Cosmet. Sci. 40, 207–216.
Hirao, T., 2003. Involvement of transglutaminase in ex vivo maturation of cornified envelopes in the stratum corneum. Int. J. Cosmet. Sci. 25, 245–257.
Hu, Z., Li, G., Xie, H., Hua, T., Chen, P., Huang, F., 2010. Measurement of Young's modulus and Poisson's ratio of human hair using optical techniques. In: Quan, C., Qian, K., Asundi, A.K., Chau, F.S. (Eds.), Society of Photo-Optical Instrumentation Engineers (SPIE) Conference Series: Pro SPIE 75222Q.
Kottner, J., Cuddigan, J.E., Carville, K., Balzer, K., Berlowitz, D., Law, S., Litchford, M., Mitchell, P., Moore, Z., Pittman, J., Sigaudo-Roussel, D., Chang, Y.Y., Haesler, E., 2020. Pressure ulcer/injury classification today: an international perspective. J. Tissue Viability 29, 197–203.
Lademann, J., Jacobi, U., Surber, C., Weigmann, H.-J., Fluhr, J.W., 2009. The tape stripping procedure – evaluation of some critical parameters. Eur. J. Pharm. Biopharm. 72, 317–323.
Levi, K., Weber, R.J., Do, J.Q., Dauskardt, R.H., 2010. Drying stress and damage processes in human stratum corneum. Int. J. Cosmet. Sci. 32, 276–293.
Levi, K., Dauskardt, R.H., 2012. Biomechanics of the barrier function of human stratum corneum. In: Treatment of Dry Skin Syndrome: the Art and Science of Moisturizers. Springer Berlin Heidelberg.
Leyva-Mendivil, M.F., Page, A., Bressloff, N.W., Limbert, G., 2015. A mechanistic insight into the mechanical role of the stratum corneum during stretching and compression of the skin. J. Mech. Behav. Biomed. Mater. 49, 197–219.
Lipsky, Z.W., German, G.K., 2019. Ultraviolet light degrades the mechanical and structural properties of human stratum corneum. J. Mech. Behav. Biomed. Mater. 100, 103391.
Liu, X., German, G.K., 2015. The effects of barrier disruption and moisturization on the dynamic drying mechanics of human stratum corneum. J. Mech. Behav. Biomed. Mater. 49, 80–89.
Liu, X., Cleary, J., German, G.K., 2016. The global mechanical properties and multi-scale failure mechanics of heterogeneous human stratum corneum. Acta Biomater. 43, 78–87.
Murahata, R.I., Crowe, D.M., Roheim, J.R., 1984. Evaluation of hydration state and surface defects in the stratum corneum: comparison of computer analysis and visual appraisal of positive replicas of human skin. J. Soc. Cosmet. Chem. 35, 327–338.
Nakagawa, H., Oyama, T., 2019. Molecular basis of water activity in glycerol-water mixtures. Front. Chem. 7, 731.
Norlén, L., 2006. Stratum corneum keratin structure, function and formation - a comprehensive review. Int. J. Cosmet. Sci. 28, 397–425.
Norlén, L., Emilson, A., Forslind, B., 1997. Stratum corneum swelling. Biophysical and computer assisted quantitative assessments. Arch. Dermatol. Res. 289, 506–513.
Oliver, W.C., Pharr, G.M., 1992. An improved technique for determining hardness and elastic modulus using load and displacement sensing indentation experiments. J. Mater. Res. 7, 1564–1583.
Oliver, W.C., Pharr, G.M., 2004. Measurement of hardness and elastic modulus by instrumented indentation: advances in understanding and refinements to methodology. J. Mater. Res. 19, 3–20.
Park, A., Baddiel, C., 1972a. Rheology of stratum corneum-I: a molecular interpretation of the stress-strain curve. J. Soc. Cosmet. Chem. 23, 3–12.
Park, A., Baddiel, C., 1972b. Rheology of stratum corneum. II. A physico-chemical investigation of factors influencing the water content of the corneum. J. Soc. Cosmet. Chem. 23, 13–21.
Park, A.C., Baddiel, C.B., 1972c. The effect of saturated salt solutions on the elastic properties of stratum. J. Soc. Cosmet. Chem. 23, 471–479.
Popov, V.L., Heß, M., Willert, E., 2019. Normal contact without adhesion. In: Popov, V.L., Heß, M., Willert, E. (Eds.), Handbook of Contact Mechanics: Exact Solutions of Axisymmetric Contact Problems. Springer, Berlin, Heidelberg, pp. 5–65.
Richter, T., Peuckert, C., Sattler, M., Koenig, K., Riemann, I., Hintze, U., Wittern, K.-P., Wiesendanger, R., Wepf, R., 2004. Dead but highly dynamic–the stratum corneum is divided into three hydration zones. Skin Pharmacol. Physiol. 17, 246–257.
Riethmuller, C., McAleer, M., Koppes, S., Abdayem, R., Franz, J., Haftek, M., Campbell, L., MacCallum, S., McLean, W., Irvine, A., Kezic, S., 2015. Filaggrin breakdown products determine corneocyte conformation in patients with atopic dermatitis. J. Allergy Clin. Immunol. 136, 1573–1580.
Rougier, A., Lotte, C., Corcuff, P., Maibach, H.I., 1988. Relationship between skin permeability and corneocyte size according to anatomic site, age, and sex in man. J. Soc. Cosmet. Chem. 39, 15–26.
Saramito, P., 2009. A new elastoviscoplastic model based on the Herschel–Bulkley viscoplastic model. J. Non-Newtonian Fluid Mech. 158, 154–161.
Takada, S., Naito, S., Sonoda, J., Miyauchi, Y., 2012. Noninvasive in vivo measurement of natural moisturizing factor content in stratum corneum of human skin by attenuated total reflection infrared spectroscopy. Appl. Spectrosc. 66, 26–32.
Warner, R.R., Stone, K.J., Boissy, Y.L., 2003. Hydration disrupts human stratum corneum ultrastructure. J. Invest. Dermatol. 120, 275–284.
Watkinson, A., Harding, C., Moore, A., Coan, P., 2001. Water modulation of stratum corneum chymotryptic enzyme activity and desquamation. Arch. Dermatol. Res. 293, 470–476.
Wildnauer, R.H., Bothwell, J.W., Douglass, A.B., 1971. Stratum corneum biomechanical properties I. Influence of relative humidity on normal and extracted human stratum corneum. J. Invest. Dermatol. 56, 72–78.
Yokouchi, M., Atsugi, T., vanLogtestijn, M., Tanaka, R.J., Kajimura, M., Suematsu, M., Furuse, M., Amagai, M., Kubo, A., 2016. Epidermal cell turnover across tight junctions based on Kelvin's tetrakaidecahedron cell shape. elife 5, e19593.
Yu, Y., Yang, W., Wang, B., Meyers, M.A., 2017. Structure and mechanical behavior of human hair. Mater. Sci. Eng., C 73, 152–163.
Yuan, Y., Verma, R., 2006. Measuring microelastic properties of stratum corneum. Colloids Surf. B Biointerfaces 48, 6–12.
Zhang, Z., Saunders, R., Thomas, C.R., 1999. Mechanical strength of single microcapsules determined by a novel micromanipulation technique. J. Microencapsul. 16, 117–124.